

# A MOLECULAR DYNAMICS SIMULATION STUDY OF THE MELTING BEHAVIOUR OF IRIDIUM NANOPARTICLES

Unal Domekeli<sup>1,\*</sup>, Arda Kolcular<sup>2</sup>,

<sup>1</sup>Dept. of Physics, Trakya University, 22030, Edirne – Türkiye <sup>2</sup>Dept. of Physics, Institute of Science, Trakya University, 22030, Edirne – Türkiye \*Corresponding author: unaldomekeli@trakya.edu.tr

#### **Abstract**

Metallic nanoparticles, which have been the focus of interest of many researchers in recent years, have many unique mechanical, electronic, optical, catalytic and thermodynamic properties, unlike their bulk forms, due to their high surface-to-volume atom ratios. Because of these properties, they are used in many application areas of materials science and nanotechnology. In this study, the melting behavior of Iridium (Ir) nanoparticles was investigated by using molecular dynamics simulation. MD simulation offers a rich analysis capability to characterize the complex melting behavior of nanoparticles at the atomic and molecular level. In order to determine the effective factors on the melting mechanism of Ir nanoparticles, thermodynamic quantities such as potential energy, heat capacity, melting temperature and melting enthalpy of the system as well as structural and dynamic properties such as pair distribution function and self-diffusion coefficients were calculated. The results indicate that particle size plays a significant role in the melting behavior of Ir nanoparticles and that melting occurs in two stages. First, the nanoparticle undergoes pre-melting, forming a liquid-like layer on the surface of the particle, and after the thickness of this layer reaches a critical value, the core region of the particle melts homogeneously.

**Keywords:** Ir nanoparticles, MD simulations, EAM potentials, melting mechanism, pre-melting.

#### INTRODUCTION

Metallic nanoparticles (NPs) attracted considerable attention in recent years due to their unique physical and properties, which chemical significantly from their bulk counterparts [1,2]. The ability to tailor the size, shape, and surface chemistry of NPs allows for precise control of their interactions at the nanoscale. This property of metallic NPs has led to innovative solutions in many areas of materials science and nanotechnology [3–5]. Therefore, further research is needed on the structural properties, thermal stability and melting behavior of metallic nanoparticles in order to control their size. Although techniques provide experimental information, they generally have limited ability to observe and predict nanometerscale phenomena, especially under conditions such as high temperature and pressure. MD simulations are a powerful tool for effortlessly providing information about the atomic-structure, dynamics, and behavior of metallic NPs [6]. Ir metal's unique combination of high density, and exceptional hardness, excellent corrosion resistance makes it an ideal material for a wide range of demanding applications, from catalysts to electronic devices to aerospace and medical fields. When Ir metal is reduced to the nanoscale, its surface area, reactivity, and catalytic properties are greatly increased. Ir NPs, in particular, have significant potential in the fields of catalysis, energy, and medicine due to their unique properties. Ir NPs were synthesized in different sizes and shapes by

reduction of Ir ions under ultraviolet irradiation [7-9]. The size and shape effect has a strong influence on the melting and scaling behavior of Ir NP near the melting temperature [10]. Therefore, Ir NPs are important for many chemical and physical applications. Despite having strong potential for many applications, there are limited studies in the literature on Ir NPs [7–13]. Taherkhani et al. [10] investigated the surface energies, melting and Debye diffusion temperatures and scaled coefficients of Ir nanoclusters with different sized truncated octahedron, octahedron, and face-centered cubic cubic geometric structures using MD simulation. They reported that the surface energy of Ir nanoclusters is largest for the truncated octahedral geometric structure and smallest for the fcc structure, and the scaling behavior of the self-diffusion coefficient near the critical temperature for different shows nanocluster shapes different behaviors. Taherkhani [13] examined the size and shape effects on the structural properties and phonon density of Ir nanoparticles using density functional theory and MD simulation. They indicated that the obtained mechanical properties and phonon density of states were in good agreement with the experimental results. In this study, the thermodynamic, structural and dynamic properties of Ir nanoparticles during heating processes were investigated detail using MD simulation with embedded atom potentials (EAM).

### **EXPOSITION**

The DLPOLY parallel code simulation package [14] was used to perform all MD simulations for Ir NPs and bulk systems. Additionally, the Ovito [15] visualization analysis program was used to process the raw data obtained as a result of MD simulation calculations. Metallic systems can be accurately described by interatomic interactions, which are often modeled in MD simulations using EAM potentials. In the EAM model, the total energy of a system

consisting of N atoms is expressed as follows [16]:

$$E_{T} = \sum_{i=1}^{N} \left[ \frac{1}{2} \sum_{i \neq j}^{N} \phi(r_{ij}) + F_{i}(\rho_{i}) \right]$$
 (1)

where  $\phi(r_{ij})$  and  $F_i(\rho_i)$  are the pairinteraction potential energy function and the embedding energy function, respectively.  $\rho_i$ is the sum of the atomic charge densities of the neighboring atoms surrounding atom  $i. r_{ij}$ is the distance between atoms i and j. In this study, the EAM potential dataset developed by Sheng [17] was used to identify Ir-Ir interactions. To investigate the size effect on the melting behavior of Ir NPs, five different spherical NPs with different diameters and number of atoms were used. Each spherical NP was extracted from an ideal fcc crystal structure with dimensions of  $50a_0 \times 50a_0 \times$  $50a_0$  ( $a_0 = 3.84$  Å for Ir [18]) using a series of spherical cutoff radii. The number of atoms and the diameters of the model NPs are listed in Table 1.

**Table 1.** The diameter (d) and number of atoms (N) of Ir NPs.

Symbol	d (nm)	Number of atoms ( <i>N</i> )
NP-1	2.5	603
NP-2	4.3	2491
NP-3	6.0	8007
NP-4	8.0	19069
NP-5	10.0	36465

The NPs were simulated using the NVT ensemble under constant volume and temperature, without periodic boundary conditions. The bulk system, meanwhile, was simulated using the NPT ensemble under constant temperature and pressure, with periodic boundary conditions. The Newtonian equations of motion were using Leapfrog-Verlet integrated the algorithm, with a time step of 1 femtosecond (fs). The temperature and pressure of the system were controlled by the Nose-Hoover thermostat [19] and the Berendsen barostat [20], respectively. The stable structure at 0 K was obtained by first annealing the initial configuration at T=300 K using 100000 MD time steps, followed by cooling to T = 0 K at a rate of 0.05 K/ps. For each NP and bulk system, the temperature was increased in a series of MD simulations by  $\Delta T$ = 100 K, and then reduced to  $\Delta T$ =10 K around the melting point to account for large temperature fluctuations. Simulations were performed at each temperature for 100000 MD time steps. The first 50000 MD time steps were used to equilibrate the system, and the final 50000 MD time steps were used to generate the time-averaged features.

In the results section, firstly, to test the EAM potential used to describe interatomic interactions in MD simulations, some physical properties of bulk Ir such as lattice constant ( $a_0$ ), cohesive energy ( $E_c$ ), melting temperature ( $T_m$ ), heat of fusion ( $\Delta H_m$ ) were calculated and the results are given in Table 2 in comparison with the experimental values. MD results are in good agreement with experimental results.

Table 2. Physical properties for bulk Ir.

Bulk system	MD	Experimental
<i>a</i> <sub>o</sub> (Å)	3.84	3.84ª
$E_{c}$ (eV)	6.94	$6.94^{a}$
$T_{m}\left(K\right)$	2550	2720 <sup>a</sup>
$\Delta H_m \left( kJ/mol \right)$	43.15	41.12

a [18]

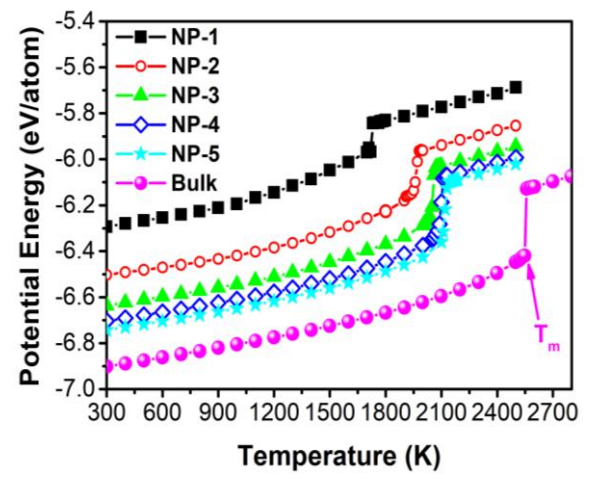


Fig. 1. Temperature-dependence of potential energy for Ir NPs and bulk system.

The most effective method of determining the first-order phase transition of NPs and the bulk system is to examine the changes in thermal properties, such as potential energy and heat capacity  $(C_p)$ , as a function of temperature. Figure 1 shows the change in potential energy with temperature for Ir NPs and the bulk. The potential energy curve for each system exhibits a linear increase with increasing temperature. The energy curve shows a sudden increase at the temperature defined as the melting point. This behavior observed in the energy curve is a significant indicator that the system has undergone a first-order phase transition. Above the melting point, the energy curve remains linear with temperature. Furthermore, the potential energy of all NPs is higher than that of bulk systems due to their high surface energy. However, as particle size increases, potential energy decreases. Figure 2 shows the temperature-dependent changes in the calculated  $C_p$  for Ir NPs and bulk. For each system, the slope of the  $C_p$  curves increases sharply at the temperature at which a sudden increase in potential energy is observed. This behavior clearly indicates that the system is undergoing a first-order phase transition. Furthermore, for all systems,  $C_p$  tends to the value  $(C_p \approx 25$ **Dulong-Petit** J/molK) expected for harmonic solids at room temperature.

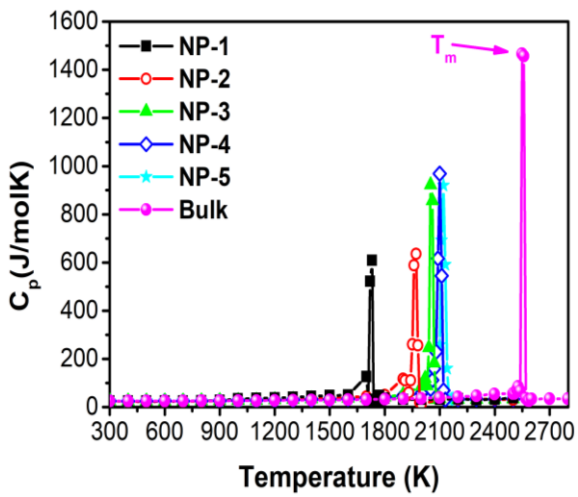
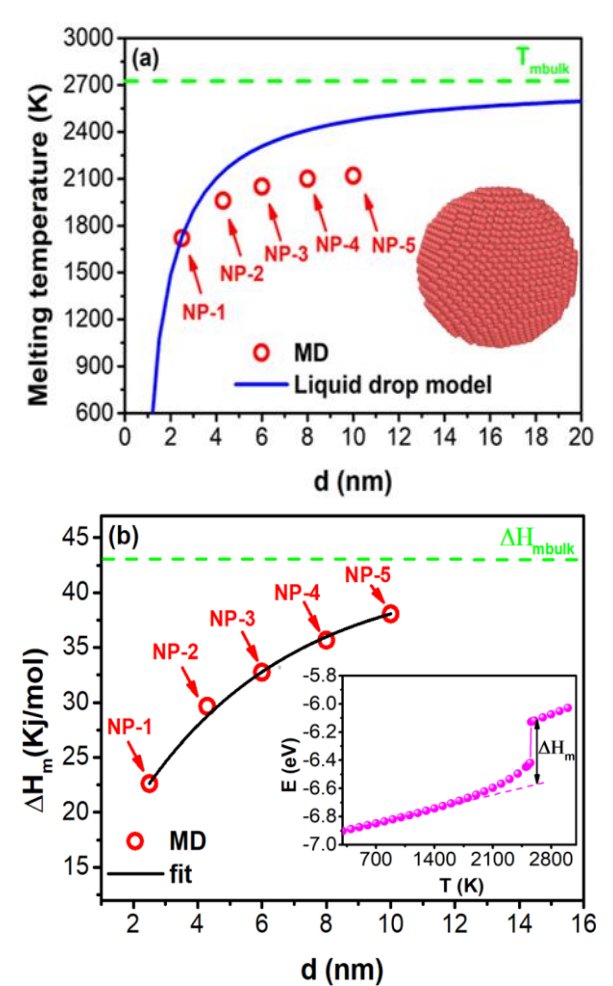


Fig. 2. Temperature-dependence of heat capacity for Ir NPs and bulk system.

The changes in  $T_m$  and  $\Delta H_m$  values obtained from the caloric curves for Ir NPs depending on particle size are given in

Figure 3. The  $T_m$  values obtained from the MD simulation are compared with the values calculated with the liquid drop model [21] in Figure 3a. While the MD results show good agreement with the liquid drop model at small sizes, this agreement deteriorates at larger sizes.  $T_m$  increases as the particle diameter increases.



**Fig. 3.** The change in the  $T_m$  and  $\Delta H_m$  values of Ir NPs depending on particle diameter.

The pair distribution function (PDF) is the most important structural function that is frequently used to analyze structural properties. The PDF, g(r), is as follows [16]:

$$g(r) = \frac{\Omega}{N^2} \left\langle \sum_{i}^{N} \sum_{i \neq j}^{N} \delta(r - r_{ij}) \right\rangle$$
 (2)

where N and  $\Omega$  represent the number of atoms, and volume of the simulations cell, respectively. Figure 4 shows the PDFs of Ir NP-3 at various temperatures. At 300 K, the PDF exhibits the characteristic behavior of

an ideal fcc crystal structure. The peak amplitudes of the PDF decrease with increasing temperature, while the peak widths increase. At 2060 K, the PDF exhibits the behavior characteristic of a liquid phase. At its melting point of 2050 K, however, it exhibits the behavior characteristic of both a solid and a liquid phase coexisting. These results support the melting point predicted from the caloric curves.

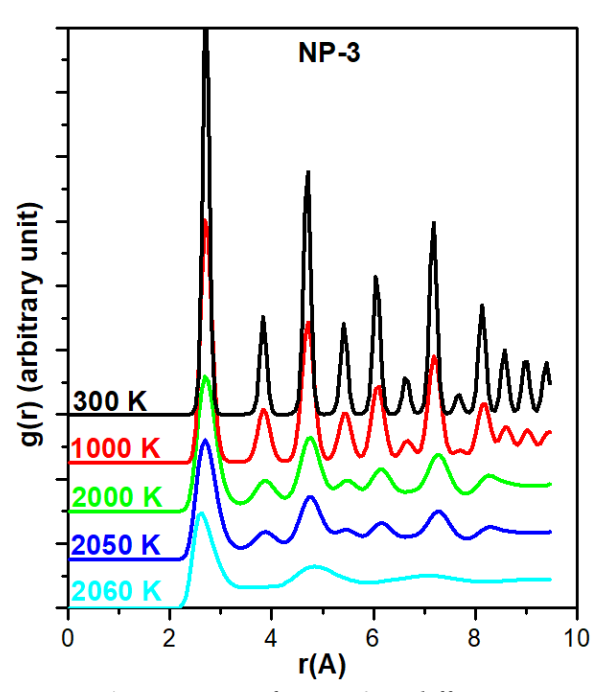


*Fig. 4.* PDFs of Ir NP-3 at different temperatures during the heating process.

To explain the melting phenomenon of NP-3, the spherical nanoparticle was divided into six regions, each consisting of five spherical shells and cores, each with a thickness of  $a_o$ . The spherical shells are labeled, from outermost to innermost, as Alayer, B-layer, C-layer, D-layer, E-layer, and core (see Figure 5). As shown in Figure 5, at 100 K, the atoms in each layer and core are in fcc crystal lattice positions. The atoms in each region maintain their current positions until 1860 K. At 1860 K, the metallic bonds between the atoms in the A-layer break, and the atoms move away from the lattice points, forming a liquid layer in the outermost region of the NP. However, the other layer and core atoms maintain their current fcc crystal structure. At 2040 K, the liquid layer

formed in the outermost layer extends into the interior of the NP, and the B-layer also melts. However, the other regions still retain their crystal structure. At 2060 K, in addition to the A- and B-layers, the C-, D-, and E-layers and the core melt, and the NP transitions completely to the liquid phase.

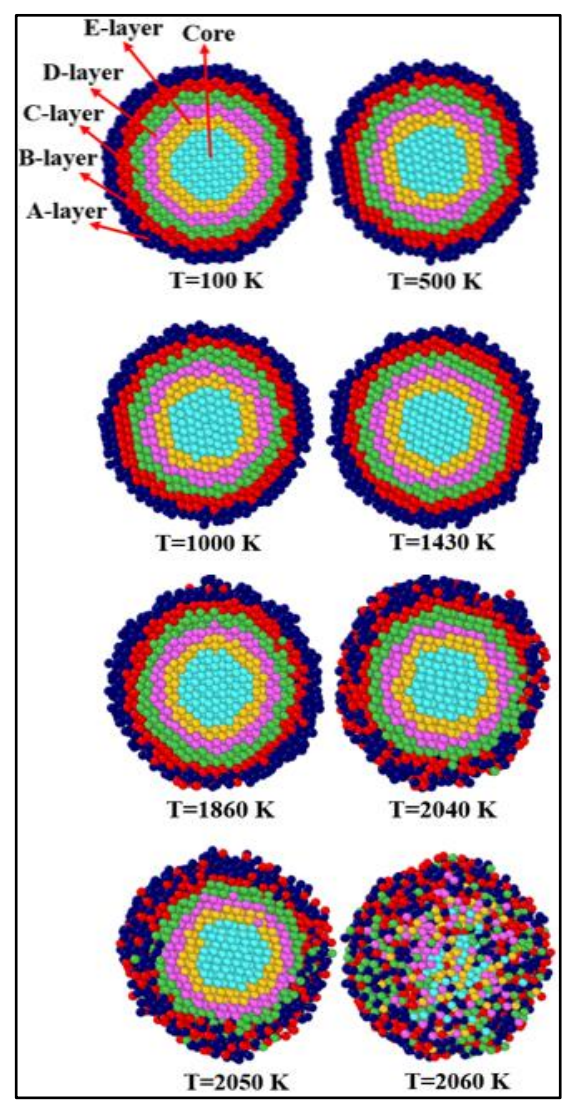


Fig. 5. Snapshots of the projected atomic positions of NP-3 during the heating process.

Self-diffusion coefficients were calculated to observe the atomic mobility in each region of NP-3. The self-diffusion coefficient, *D*, is calculated by using the Einstein equation [22]:

$$D = \lim_{t \to \infty} \frac{MSD}{6t} \tag{3}$$

where *t* is the diffusion time, MSD of the atom in the MD simulations can be described as [22]:

$$MSD = \frac{1}{N} \sum_{i=1}^{N} |r_i(t + t_o) - r_i(t_o)|^2$$
 (4)

where  $r_i(t_o)$  is the position vector of the *i*th for the system in atom its initial configuration and  $r_i(t)$  is the position vector of ith atom at time t. The temperaturedependent changes of the self-diffusion coefficients calculated for each region of NP-3 are given in Figure 6. The selfdiffusion coefficients of the A-, B-, C-, Dand E-layers, as well as the core, are around zero up to approximately 1430 K. An increase in the self-diffusion coefficient of the A-layer begins to be observed at this temperature, indicating that the A-layer is beginning to melt. At 1860 K, an increase in the self-diffusion coefficients of the B-layer begins in addition to the A-layer. However, the self-diffusion coefficients of the C-, D-, and E-layers and the core are still around zero.

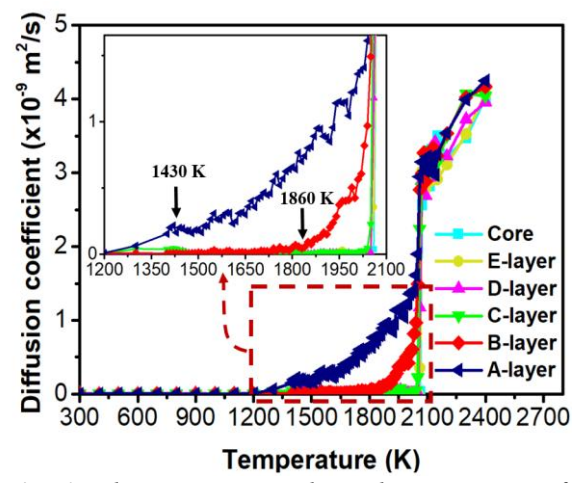


Fig. 6. The temperature-dependent variation of the self-diffusion coefficients of NP-3.

## **CONCLUSION**

In this study, we have investigated the melting behavior of Ir nanoparticles using molecular dynamics simulation with EAM force field. MD simulation results indicate that particle size plays an important role in the melting behavior of Ir nanoparticles. As particle size increases,  $T_m$  and  $\Delta H_m$  increase, while potential energy decreases. The  $T_m$  and  $\Delta H_m$  values of all NPs are smaller than those of the bulk. The melting mechanism of NP-3 occurs in two stages. First, the

nanoparticle undergoes pre-melting, forming a liquid-like layer on its surface. Once this layer has reached a critical thickness  $(2a_o)$ , the particle melts homogeneously.

Funding No funding support has been received from any institution or person.
Acknowledgments: We would like to thank Trakya University Rectorate for giving permission and contributing to present this study as a paper.

#### REFERENCE

- [1] J. Mackerle, Nanomaterials, nanomechanics and finite elements: a bibliography (1994–2004), Model. Simul. Mater. Sci. Eng. 13 (2005) 123–158.
- [2] E.L. Wolf, Nanophysics and Nanotechnology, Wiley, 2006.
- [3] S.H. Joo, J.Y. Park, J.R. Renzas, D.R. Butcher, W. Huang, G.A. Somorjai, Size Effect of Ruthenium Nanoparticles in Catalytic Carbon Monoxide Oxidation, Nano Lett. 10 (2010) 2709–2713.
- [4] Y. Yan, S.C. Warren, P. Fuller, B.A. Grzybowski, Chemoelectronic circuits based on metal nanoparticles, Nat. Nanotechnol. 11 (2016) 603–608.
- [5] R. Ferrando, J. Jellinek, R.L. Johnston, Nanoalloys: From Theory to Applications of Alloy Clusters and Nanoparticles, Chem. Rev. 108 (2008) 845–910.
- [6] W.C. Ng, T.L. Lim, T.L. Yoon, Investigation of Melting Dynamics of Hafnium Clusters, J. Chem. Inf. Model. 57 (2017) 517–528.
- [7] G.S. Fonseca, G. Machado, S.R. Teixeira, G.H. Fecher, J. Morais, M.C.M. Alves, J. Dupont, Synthesis and characterization of catalytic iridium nanoparticles in imidazolium ionic liquids, J. Colloid Interface Sci. 301 (2006) 193–204.
- [8] E. Redel, J. Krämer, R. Thomann, C. Janiak, Synthesis of Co, Rh and Ir nanoparticles from metal carbonyls in ionic liquids and their use as biphasic liquid–liquid hydrogenation nanocatalysts for cyclohexene, J. Organomet. Chem. 694 (2009) 1069–1075.
- [9] S. Kundu, H. Liang, Shape-selective formation and characterization of catalytically active iridium nanoparticles, J. Colloid Interface Sci. 354 (2011) 597–606.

- [10] F. Taherkhani, F. Taherkhani, Ir nanocluster shape effects on melting, surface energy and scaling behavior of self-diffusion coefficient near melting temperature, Comput. Mater. Sci. 201 (2022) 110935.
- [11] T. Pawluk, L. Wang, Molecular Dynamics Simulations of the Coalescence of Iridium Clusters, J. Phys. Chem. C 111 (2007) 6713–6719.
- [12] S. Singha, E. Serrano, S. Mondal, C.G. Daniliuc, F. Glorius, Diastereodivergent synthesis of enantioenriched α,βdisubstituted γ-butyrolactones via cooperative N-heterocyclic carbene and Ir catalysis, Nat. Catal. 3 (2019) 48–54.
- [13] F. Taherkhani, Size and shapes effect on structural and phonon density of state in Ir nanoparticle and mechanical properties of Ir metal, Comput. Mater. Sci. 237 (2024) 112893.
- [14] W. Smith, T.R. Forester, DLPOLY 2.0: A general-purpose parallel molecular dynamics simulation package, J. Mol. Graph. 14 (1996) 136–141.
- [15] A. Stukowski, Visualization and analysis of atomistic simulation data with OVITO—the Open Visualization Tool, Model. Simul. Mater. Sci. Eng. 18 (2010) 015012.
- [16] U. Domekeli, M. Celtek, Structural and dynamic properties of aluminum nanoparticles during the melting process, UNITECH 2024 Sel. Pap. (2024).
- [17] H. Sheng, EAM potentials, (2025). https://sites.google.com/site/eampotentials/table/ir.
- [18] C. Kittel, Introduction to the physics of the solid state, University, John Wiley & Sons, Inc, 1986.
- [19] S. Nose, A unified formulation of the constant temperature molecular dynamics methods, J. Chem. Phys. 81 (1984) 511–519.
- [20] H.J.C. Berendsen, J.P.M. Postma, W.F. van Gunsteren, A. DiNola, J.R. Haak, Molecular dynamics with coupling to an external bath, J. Chem. Phys. 81 (1984) 3684–3690.
- [21] K.K. Nanda, Size-dependent melting of nanoparticles: Hundred years of thermodynamic model, Pramana 72 (2009) 617–628.
- [22] U. Domekeli, M. Celtek, Melting mechanism of cylindrical molybdenum nanowire: a molecular dynamics simulation study, UNITECH 2024 Sel. Pap. (2024).